Multimode interference tapered fiber refractive index sensors

Claudecir R. Biazoli,[1] Susana Silva,[2] Marcos A. R. Franco,[3] Orlando Frazão,[2] and Cristiano M. B. Cordeiro[1,*]

[1]Instituto de Física "Gleb Wataghin," Universidade Estadual de Campinas—UNICAMP, Campinas, São Paulo, Brazil

[2]INESC-Porto, Rua do Campo Alegre 687, 4169-007 Porto, Portugal

[3]Instituto de Estudos Avançados, São José dos Campos, São Paulo, Brazil

*Corresponding author: cmbc@ifi.unicamp.br

Received 4 April 2012; revised 27 June 2012; accepted 6 July 2012; posted 9 July 2012 (Doc. ID 163487); published 20 August 2012

Real-time monitoring of the fabrication process of tapering down a multimode-interference-based fiber structure is presented. The device is composed of a pure silica multimode fiber (MMF) with an initial 125 μm diameter spliced between two single-mode fibers. The process allows a thin MMF with adjustable parameters to obtain a high signal transmittance, arising from constructive interference among the guided modes at the output end of the MMF. Tapered structures with waist diameters as low as 55 μm were easily fabricated without the limitation of fragile splices or difficulty in controlling lateral fiber alignments. The sensing device is shown to be sensitive to the external environment, and a maximum sensitivity of 2946 nm/refractive index unit in the refractive index range of 1.42–1.43 was attained.

OCIS codes: 060.2370, 060.2270.

1. Introduction

The multimode interference (MMI) concept has been comprehensively studied in the past few years in order to develop new optical devices [1]. Typically, the MMI-based fiber device consists of a step-index multimode fiber (MMF) section spliced between two single-mode fibers (SMFs), forming an SMF–MMF–SMF (SMS) structure [2]. The light coming from the input SMF excites several modes of the MMF section, thus causing interference between them along the fiber. The coupling efficiency to the output SMF will depend on the amplitudes and relative phases of the several modes at the exit end of the MMF; therefore, distinct field profiles will appear in accordance with the length L of the MMF section used. The self-imaging effect [3] is a periodic condition found along the direction of propagation as well as where field condensation occurs due to constructive interference between all guided modes. As a result, the light field at the input of the MMF section is replicated for a specific wavelength in both amplitude and phase on its output, thus providing a bandpass spectral peak. Several applications can be found where the MMI-based fiber devices rely on the self-imaging concept: fixed-wavelength [4] and tunable wavelength [5] bandpass filtering, fiber lasers [6], and measurement of temperature [7], liquid level [8], refractive index [9], and displacement [10]. MMI structures can also be used in active devices, e.g., to improve the gain saturation level and heat dissipation ability due the large modal area in a superluminescent light emitting diode (SLED) [11,12].

Despite the simplicity of such fiber devices, they often require enhancement of sensitivity when used in specific applications such as in refractometry. The most common solution is to chemically etch the MMF section of the SMS structure in order to increase sensitivity to the external medium [13]. A simple

1559-128X/12/245941-05$15.00/0

solution to avoid the etching process is to use instead a coreless MMF, i.e., a pure silica fiber, spliced between the two SMFs, thus forming MMI. In this line of research, Silva *et al.* [14] reported a highly sensitive temperature sensor based on the self-imaging effect that occurred in the coreless MMF of the SMS fiber structure, where several MMF diameters were used. Optimized results were achieved for the coreless MMF with the smallest diameter (i.e., 55 μm) in a high sensitivity refractive index (RI) range. Therefore, by decreasing the MMF diameter, an increase of sensitivity to the surrounding medium could be achieved. However, in this case, the disadvantage arises from the need to perform difficult splices between SMFs and MMFs with smaller diameters (far below 125 μm).

A different approach to overcome this limitation is the tapered fiber structure. Recently, Wang *et al.* [15,16] proposed and experimentally demonstrated an evanescent field fiber refractometer relying on a tapered SMS fiber structure. The device was composed of a standard 105/125 μm MMF spliced between two SMFs. In [15], a CO_2 laser was employed to fabricate a short tapered MMF section with a waist diameter and length of approximately 30 and 675 μm, respectively, with no control or optimization of the taper dimensions, nor was the spectral profile rigorously controlled.

This work reports the real-time monitoring of the fabrication process of a tapered SMS fiber structure. The device relies on a coreless MMF (pure silica rod), part of which was tapered down by flame brushing technique [17,18], spliced between two SMFs. The temporal evolution of the transmittance signal versus wavelength is presented, when reducing the MMF in the interval from 80 to 40 μm. It is shown that the shape of the tapered device could be controlled, as well as the desired optical spectrum. By doing so, the bandpass peak (arising from constructive interference, i.e., self-imaging) can be adjusted to appear in the desired wavelength region. An alternative optical sensor device based on the interaction of the evanescent field that surrounds the MMF waist with the external environment is shown. This solution is more robust, since it eliminates the need for difficult splices to fibers with smaller diameters when the purpose is to increase sensitivity with the external medium [13,14]. The tapered structure was immersed in different RI liquids in the range 1.30–1.42, and its sensitivity was ascertained.

2. Multimode Tapered Devices: Fabrication, Characterization, and Modeling

The fiber device developed and studied in this work is based on a tapered coreless MMF spliced between two SMFs, thus forming a tapered SMS fiber structure. The taper was made in a section of MMF by the flame brushing technique. The fabrication involves heating a well defined portion of fiber with a localized flame (approximately 4 mm), while applying a tensile force by pulling the fiber with translation stages, each one having submicrometer resolution. The MMF has an initial total length (L_{Total}) of 20 mm, 18 mm of it being tapered down to form the fiber transition regions (Z) and the taper waist (with length L_w and diameter D_w); see Fig. 1. As the fiber elongates, its cross-sectional area is reduced accordingly. The transition regions can have a controllable shape [18], being linear in the tapered structures presented here. Other transition shapes, such as exponential, are currently being studied, with expected influence in the number of guided modes and, in consequence, the bandwidth of the spectral peaks [16].

Figure 1 shows the details of the tapered device and the experimental characterization setup. The fiber structure was interrogated in transmission by means of a broadband light source (a SLED) in the 1550 nm spectral range and an optical spectrum analyzer (OSA), or by a 1550 nm distributed feedback (DBF) laser and a power meter (see Fig. 1). Therefore, the fabrication process of tapering down the coreless MMF was monitored in real time, and by controlling the MMF diameter, constructive interference peaks were attained in the spectral region 1500–1700 nm. The temporal evolution of the transmittance signal versus wavelength was also recorded during this process.

Figure 2(a) shows the experimental optical spectra of the tapered structure when the diameter is reduced from the original 125 μm to 74 μm ($L_w \sim 10.7$ mm). One notices a bandpass peak related to the constructive interference among the guided modes at 1550 nm, with a transmittance greater than 70%.

To model such a structure [see Fig. 2(a) inset], commercial software based on a three-dimensional wide-angle scalar beam propagation method (BPM; Rsoft Design) was used. A tapered MMF section (pure silica rod) with a 74 μm waist diameter was considered, as well as 2 mm long SMFs for the light input and output. Here, an implicit finite-difference approach (Crank–Nicholson scheme) with Padé approximant of order 1.1 to the differential operator along the propagation direction was employed. In order to avoid spurious reflections from computational

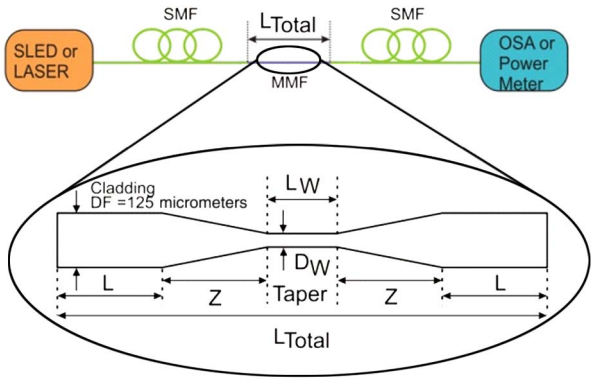

Fig. 1. (Color online) Experimental setup and details of the MMI-based tapered device. D_W, L_W, and L_{total} indicate the diameter and length of the taper waist region and the coreless MMF total length, respectively.

window edges, full transparent boundary conditions were included.

The modeling of this 74 μm thick MMF, as depicted in the Fig. 2(a) inset, shows similar behavior to the one attained experimentally. The poor quantitative agreement is due to the difficulty of knowing the exact tapered fiber parameters and the high sensitivity of the spectral results with such dimensions [as will be explored in Fig. 4(b)].

Figure 2(b) presents the results of a coreless MMF tapered down to a region close to 55 μm ($L_w \sim 8$ mm) where, again, a bandpass peak appears in the region around 1550 nm; hence, the self-imaging condition is satisfied. As the tapering process evolves [as can be noted in the online movie (Media 1)] the bandpass peak moves to shorter wavelengths. The online movie (Media 1) shows the experimental spectral evolution in the taper waist diameter range from 80 to 40 μm.

The spectral response obtained in Fig. 2(b) is similar to the one obtained for the first self-image of an SMS fiber structure formed by a coreless MMF originally with a 55 μm diameter and 11.5 mm long (no tapers) [14]. Consequently, the tapered structure has the advantage of eliminating splices to MMFs with smaller original diameters, thus avoiding possible fiber misalignments (which influence the mode coupling in the MMF) in the splicing process.

To give a general view of the bandpass peak evolution during the tapering process, Fig. 3(a) shows the plot of the field intensity along the coreless MMF section in the fixed wavelength of 1550 nm and according to the waist diameter (D_w, vertical axis) and total length (L_{Total}, horizontal axis). It should be remembered that the MMF is spliced to an SMF in both entrance and exit tips. The interface between the input SMF/MMF is shown as a vertical white dotted line, while the interface between the MMF/exit SMF is shown as a diagonal white dotted line. During tapering, as the MMF diameter decreases, the transition length (Z) increases. The interfaces indicating the final part of the input transition, as well as the initial part of the output transition, are indicated as yellow dotted lines. The region in between these lines represents the taper waist length (L_w), which is 20 mm long when the fiber is not tapered (125 μm) and 2.9 mm long when the taper waist is 20 μm. It can be observed that, as expected, the position of the bandpass peaks is more strongly affected with a reduction of the taper diameter; note that at smaller fiber diameters [close to 20 μm, bottom of Fig. 3(a)], the lines that represent the main peaks [higher intensity, green in Figs. 3(a) and 3(b)—see color scale on the right hand side] bend more than in the case of a fiber with a bigger diameter (close to 125 μm).

As the MMF is tapered down, the waist diameter reduces and the total length (L_{Total}) increases. When the waist diameter reaches 20 μm, the total length becomes 50 mm. The horizontal pink line represents checking the field profile within a tapered structure with 57.5 μm. In a different perspective, Fig. 3(b) shows the longitudinal tapered MMF profile where $Z = 14.6$ mm, $L_w = 8.3$ mm, and $L_{\text{Total}} = 39.5$ mm. On the other hand, the diagonal light green line represents the evolution of the intensity in the fiber structure end tip when tapering the MMF from 60 to 40 μm [also visible in Fig. 4(a)].

Figure 4(a) shows the transmittance, both experimental and simulated, of the device as a function of the waist diameter (D_w) in the short interval between 60 and 40 μm. As can be noted, several high transmittance peaks are presented in both sets of data. Similar to the case of Fig. 2(a), a good quantitative match between simulated and measured data is, however, difficult to obtain, mainly due to the challenge of achieving high accuracy of the taper main parameters (D_w, L_w, Z). The experimental data were attained (see Fig. 1) by monitoring the transmittance signal of a 1550 nm DBF laser with a power meter, while the coreless MMF diameter was being reduced. Figure 4(b) presents the simulation of the transmittance signal at 1550 nm when changing the MMF diameter from 55 to 53 and 57 μm. One notices that the bandpass peak changes more than 120 nm (from 1561 to 1498 and 1626 nm), showing the high sensitivity of the system to small changes in the tapered MMF dimensions. Taking advantage of the

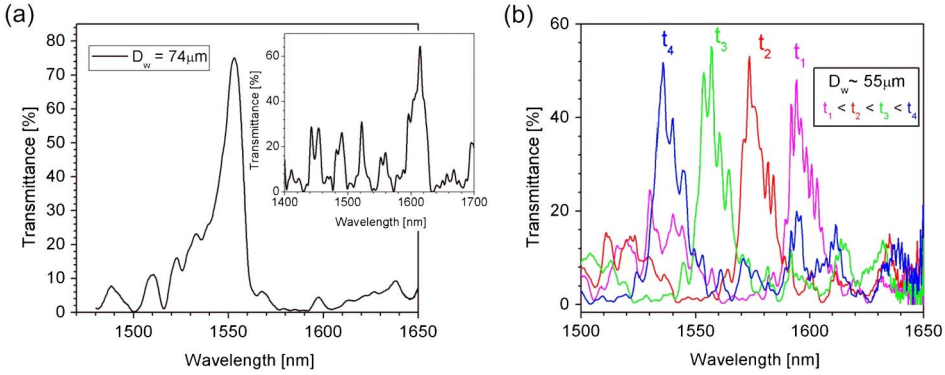

Fig. 2. (Color online) (a) Measured transmittance signal of a tapered fiber with a 74 μm diameter (inset shows the corresponding modeled result) and (b) graph superimposing different frames from the movie (Media 1; experimental data) when the diameter is being reduced in the region close to 55 μm. Movie online (Media 1): Temporal evolution of the measured transmittance signal versus wavelength when tapering down the MMF in the interval from 80 to 40 μm.

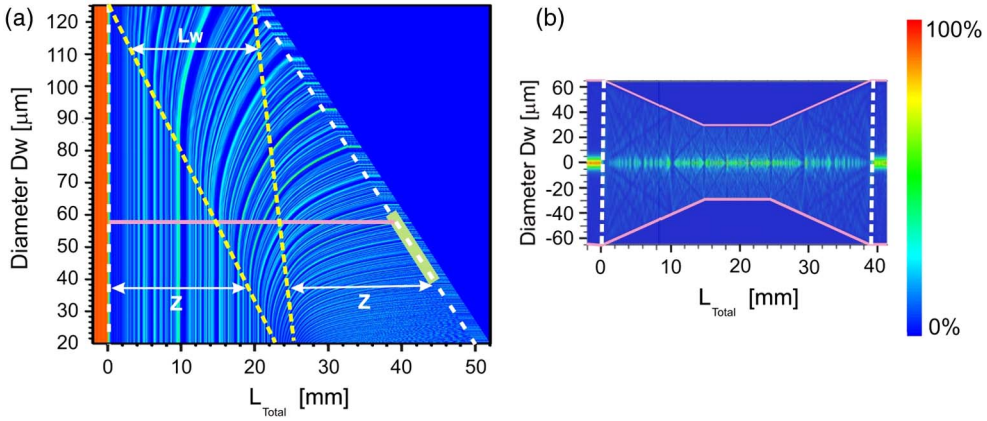

Fig. 3. (Color online) Three-dimensional plots of the optical signal intensity (color) at 1550 nm. White dotted lines represent the SMF/MMF interfaces. (a) Plot of the tapered diameter (vertical axis) versus total fiber length (horizontal axis). Yellow lines represent when the transition regions finish or start. The diagonal green line indicates the intensity in the fiber end tip from a 60 to 40 μm taper diameter, also shown in Fig. 4(a). (b) Longitudinal fiber profile with $D_w = 57.5$ μm [related with the pink line in Fig. 3(a)].

possibility of developing tapered SMS structures with small diameters, without the drawback of fragile splices [13] or the difficulty of controlling fiber alignments, the sensitivity of such devices was studied against the external RI change.

3. RI Sensor

The behavior of the tapered SMS fiber structure with a 55 μm diameter was characterized in response to external RI variations. The experiment was performed by placing the sensing device in contact with liquids with distinct RIs in the range 1.30–1.43 [Fig. 5(a), inset] at room temperature. A series of commercial RI standards from Cargille Laboratories (Cedar Grove, NJ) were used accordingly, and such standards were properly corrected for the operation wavelength of 1550 nm. The optical spectrum variation of the tapered structure with liquid RIs is depicted in Fig. 5(a).

As predicted, the signal transmittance decreases with increasing RI, since the external medium approaches the silica RI (1.44) of the coreless MMF. The wavelength shifts as well, because the effective RI of the guided modes at the tapered coreless MMF changes with RI variations of the external medium. The wavelength dependence of such fiber structure on the RI variation of the surrounding medium is presented in Fig. 5(b). As expected [13,14], the wavelength shift increases with increasing liquid RI and the behavior is not linear in the RI range studied. Analysis of the results showed that in the lower RI range of 1.30–1.33, a sensitivity of 148 nm/RIU was achieved, while in the high sensitivity RI region of 1.42–1.43, a typical value of 2946 nm/RIU was also attained. Previous results have shown that using a coreless-MMF-based SMS fiber structure with a 55 μm original diameter, sensitivities of 140 and 2800 nm/RIU for the RI ranges of 1.30–1.33 and 1.42–1.43, respectively, have been achieved [14]. It can also be noted that the peak bandwidth increases when the external RI approaches that of silica, which is expected to reduce the system resolution. This is due the reduction of the number of guided modes in the MMF.

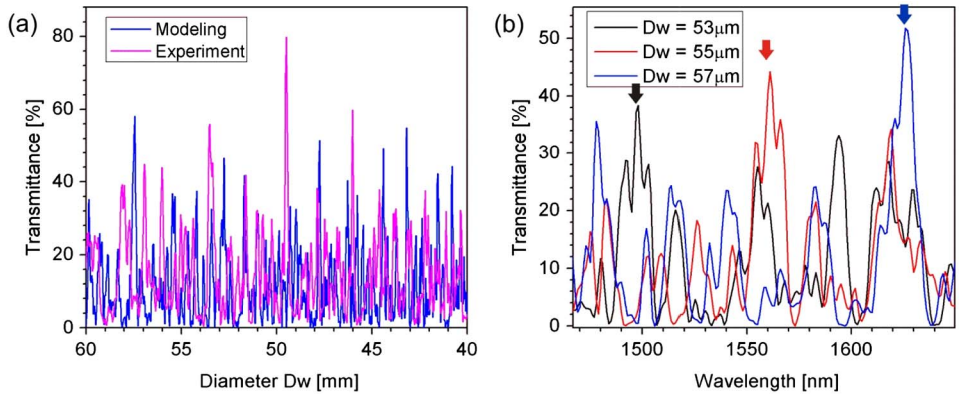

Fig. 4. (Color online) (a) Modeled and experimental transmittance signals versus taper diameter from 60 to 40 μm at 1550 nm wavelength and (b) study (simulation) of the transmittance signal when changing the taper diameter from 53 to 57 μm; arrows indicate the main peak position.

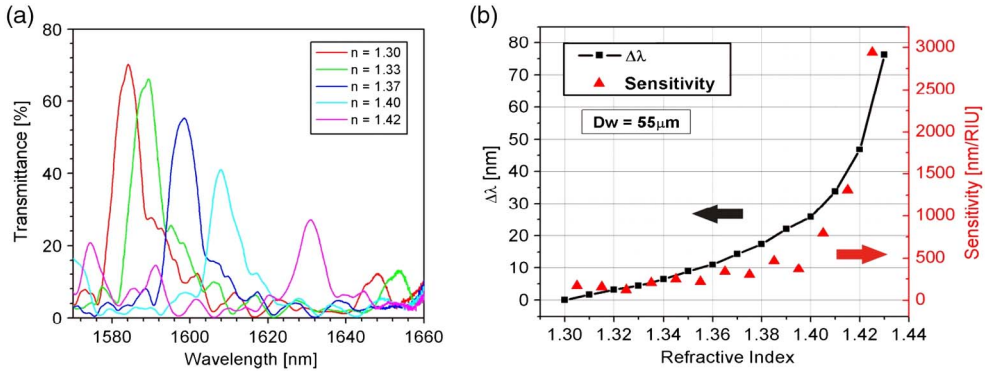

Fig. 5. (Color online) (a) Optical spectrum variation of the SMS fiber structure when changing the liquid refractive index that surrounds the tapered region with a 55 μm diameter (inset) from 1.30 to 1.43 and (b) wavelength shift (left axis) and sensitivity (right axis) versus liquid refractive index variation.

4. Conclusion

A tapered all-fiber MMI device was fabricated and characterized in real time. The MMF, a pure silica rod, had an initial diameter of 125 μm and was easily spliced between two SMFs to form an SMS-based fiber device. By monitoring in real time the transmittance signal in the range of 1450–1650 nm, it was possible to see bandpass peaks (resulting from constructive interference) and the displacement of the peaks to shorter wavelengths [check the movie file online (Media 1)] while the diameter of the taper was being reduced and elongated. Tapered structures with waist diameters as low as 55 μm were easily fabricated without the drawback of fragile splices or difficulty in controlling lateral fiber alignments. Modeling was done to support the experimental results. The sensitivity of the tapered SMS fiber device to external RI variations was also ascertained, and a maximum sensitivity of 2946 nm/RIU in the RI range of 1.42–1.43 was attained as well. Finally, with the control in real time of the taper fabrication in SMF–MMF–SMF, it is possible to fabricate structures in series with different wavelengths for simultaneous measurement of physical/chemical/biological parameters.

This work was supported by a binational collaboration project, CAPES-FCT Brazil/Portugal (# 293/11), and the Brazilian agencies FAPESP, CNPq, FINEP, and CAPES (Pró-Defesa). C. M. B. Cordeiro and C. R. Biazoli thank J. G. Hayashi for producing the multimode fiber at UNICAMP/Brazil and G. Wiederhecker for helping with the movie file.

References

1. O. Frazão, S. Silva, J. Viegas, L. A. Ferreira, F. M. Araújo, and J. L. Santos, "Optical fiber refractometry based on multimode interference," Appl. Opt. **50**, E184–E188 (2011).
2. Q. Wang, G. Farrell, and W. Yan, "Investigation on single mode-multimode-single mode fiber structure," J. Lightwave Technol. **26**, 512–519 (2008).
3. L. B. Soldano and E. C. M. Pennings, "Optical multi-mode interference devices based on self-imaging—principles and applications," J. Lightwave Technol. **13**, 615–627 (1995).
4. W. S. Mohammed, P. W. E. Smith, and X. Gu, "All-fiber multimode interference bandpass filter," Opt. Lett. **31**, 2547–2549 (2006).
5. J. E. Antonio-Lopez, A. Castillo-Guzman, D. A. May-Arrioja, R. Selvas-Aguilar, and P. L. Wa, "Tunable multimode-interference bandpass fiber filter," Opt. Lett. **35**, 324–326 (2010).
6. A. Castillo-Guzman, J. E. Antonio-Lopez, R. Selvas-Aguilar, D. A. May-Arrioja, J. Estudillo-Ayala, and P. L. Wa, "Widely tunable erbium-doped fiber laser based on multimode interference effect," Opt. Express **18**, 591–597 (2010).
7. R. X. Gao, Q. Wang, F. Zhao, B. Meng, and S. L. Qu, "Optimal design and fabrication of SMS fiber temperature sensor for liquid," Opt. Commun. **283**, 3149–3152 (2010).
8. J. E. Antonio-Lopez, J. J. Sanchez-Mondragon, P. L. Wa, and D. A. May-Arrioja, "Fiber-optic sensor for liquid level measurement," Opt. Lett. **36**, 3425–3427 (2011).
9. Q. Wu, Y. Semenova, B. Yan, Y. Ma, P. Wang, C. Yu, and G. Farrell, "Fiber refractometer based on a fiber Bragg grating and single-mode-multimode-single-mode fiber structure," Opt. Lett. **36**, 2197–2199 (2011).
10. Q. Wu, Y. Semenova, P. Wang, A. M. Hatta, and G. Farrell, "Experimental demonstration of a simple displacement sensor based on a bent single-mode—multimode—single-mode fiber structure," Meas. Sci. Technol. **22**, 025203 (2011).
11. Z. Zang, T. Minato, P. Navaretti, Y. Hinokuma, M. Duelk, C. Velez, and K. Hamamoto, "High power (>110 mW) superluminescent diodes using active multi-mode interferometer," IEEE Photon. Technol. Lett. **22**, 721–723 (2010).
12. Z. Zang, K. Mukai, P. Navaretti, M. Duelk, C. Velez, and K. Hamamoto, "Thermal resistance reduction in high power superluminescent diodes by using active multi-mode interferometer," Appl. Phys. Lett. **100**, 031108 (2012).
13. Q. Wu, Y. Semenova, P. Wang, and G. Farrell, "High sensitivity SMS fiber structure based refractometer—analysis and experiment," Opt. Express **19**, 7937–7944 (2011).
14. S. Silva, E. G. P. Pachon, M. A. R. Franco, J. G. Hayashi, F. X. Malcata, O. Frazão, P. Jorge, and C. M. B. Cordeiro, "Ultrahigh-sensitivity temperature fiber sensor based on multimode interference," Appl. Opt. **51**, 3236–3242 (2012).
15. P. Wang, G. Brambilla, M. Ding, Y. Semenova, Q. Wu, and G. Farrell, "High-sensitivity, evanescent field refractometric sensor based on a tapered, multimode fiber interference," Opt. Lett. **36**, 2233–2235 (2011).
16. P. Wang, G. Brambilla, M. Ding, Y. Semenova, Q. Wu, and G. Farrell, "Investigation of single-mode—multimode—single-mode and single-mode—tapered-multimode—single-mode fiber structures and their application for refractive index sensing," J. Opt. Soc. Am. B **28**, 1180–1186 (2011).
17. G. Brambilla, V. Finazzi, and D. J. Richardson, "Ultra-low-loss optical fiber nanotapers," Opt. Express **12**, 2258–2263 (2004).
18. T. A. Birks and Y. W. Li, "The shape of fiber tapers," J. Lightwave Technol. **10**, 432–438 (1992).